Rates and Mechanism of Biphenyl Synthesis Catalyzed by Electrogenerated Coordinatively Unsaturated Nickel Complexes

Christian Amatore* and Anny Jutand

Ecole Normale Supérieure, Laboratoire de Chimie, Unité associée au CNRS 1110, 24, rue Lhomond, 75231 Paris Cedex 05, France

Received March 15, 1988

When performed under a constant reductive driving force, the mechanism of coupling of aryl halides by nickel catalysts is found to proceed through a chain reaction involving Ni(0), Ni(I), Ni(II), and Ni(III) complexes. The propagation steps include the oxidative addition of PhBr to the electrogenerated unsaturated Ni^0(dppe). The resulting $PhNi^{II}Br$(dppe) is reduced to $PhNi^{I}$(dppe) via a single electron uptake. The latter undergoes an oxidative addition with PhBr to afford the trivalent nickel complex $Ph_2Ni^{III}Br$(dppe) which reductively eliminates Ph–Ph to yield $Ni^{I}Br$(dppe). The cycle is closed by a further single electron transfer to the monovalent nickel which restores the starting zerovalent nickel. The different steps have been characterized independently from transient electrochemical data, and the rate constants of the three chemical steps have been determined. The cycle is initiated by the two-step reduction of $Ni^{II}Cl_2$(dppe) into Ni^0(dppe), which readily reacts with bromobenzene. At low concentrations of bromobenzene, the oxidative addition of PhBr to the phenylnickel(I) complex is the rate-determining reaction, introducing then an apparent first-order dependence of the overall kinetics with PhBr. At larger concentrations the rate-determining step is the reductive elimination from $Ph_2Ni^{III}Br$(dppe) to afford the biphenyl, and the chain tends to propagate with a rate independent of PhBr concentration. The implications of the above mechanism for nonelectrochemical situations involving a reducing metal and catalytic amounts of nickel salts as the coupling reagents are discussed.

Introduction

Since the pioneering work of Semmelhack and coworkers,[1] synthetic procedures for the preparation of biaryls by the classical Ullmann reaction[2] have been supplanted by the use of zerovalent nickel reagents. Thus good yields of biphenyl from bromo- or iodobenzene are obtained in the presence of in situ generated Ni(0) from Ni(II) reduction by zinc powder (eq 1).[3] These original

$$2ArX + Ni(II) + Zn \rightarrow Ar\text{–}Ar + Ni(II) + ZnX_2 \quad (1)$$

methods, based upon stoichiometric amounts of nickel, were modified by Kumada et al.[4] using catalytic amounts of nickel salt and stoichiometric quantities of zinc (eq 2).

$$2ArX + Zn \xrightarrow{Ni(II)} Ar\text{–}Ar + ZnX_2 \quad (2)$$

More recently the method has been adapted[5] to afford nearly quantitative yields of biaryls from aryl chlorides although these latter were reported to react inefficiently under the original conditions of Semmelhack.[1] Interestingly this enhancement is related to the presence of an excess of reducing metal (Zn, Mn, Mg) which compares with the efficient electrosynthesis of arylcarboxylates,[6] biaryls,[7] or poly-*p*-phenylenes,[8] involving as the ultimate reductant, a cathode, the potential of which proved to be crucial for the success of reactions 3–5.

$$ArX + CO_2 + 2e^- \xrightarrow{Ni(II)} Ar\text{-}CO_2^- + X^- \quad (3)$$

$$2ArX + 2e^- \xrightarrow{Ni(II)} Ar\text{-}Ar + 2X^- \quad (4)$$

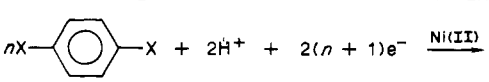

$$nX\text{–}C_6H_4\text{–}X + 2H^+ + 2(n+1)e^- \xrightarrow{Ni(II)} H\text{–}(C_6H_4)_n\text{–}H + 2nX^- \quad (5)$$

The role of the nickel reagents in the activation of the aromatic carbon–halogen bond is commonly interpreted by the involvement of arylnickel(II) intermediates formed via rapid oxidative addition of the aryl halide to in situ generated Ni(0) species.[6a,9,10] Although there is general agreement on the biaryl formation via reductive elimination from a diarylnickel species, the exact sequence of steps leading to such an intermediate from the organic halide and the initially formed arylnickel(II) is still controversial.[11]

Scheme I

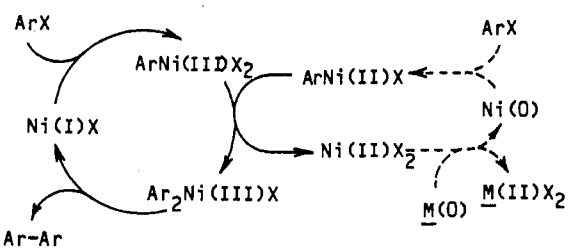

* To whom correspondence should be addressed.

(1) (a) Semmelhack, M. F.; Helquist, P. M.; Jones, L. D. *J. Am. Chem. Soc.* **1971**, *93*, 5908. (b) Semmelhack, M. F.; Ryono, L. S. *J. Am. Chem. Soc.* **1975**, *97*, 3873. (c) Semmelhack, M. F.; Helquist, P. M.; Jones, L. D.; Keller, L.; Mendelson, L.; Ryono, L. S.; Smith, J. G.; Stauffer, R. D. *J. Am. Chem. Soc.* **1981**, *103*, 6460.

(2) See, e.g.: (a) Fanta, P. E. *Chem. Rev.* **1946**, *38*, 139. (b) *Ibid.* **1964**, *64*, 613. (c) Fanta, P. E. *Synthesis* **1974**, 9. (d) Cornforth, J.; Sierakowski, A. F.; Wallace, T. W. *J. Chem. Soc., Chem. Commun.* **1979**, 294. (e) Rieke, R. D.; Rhyne, L. D. *J. Org. Chem.* **1979**, *44*, 3445. (f) Wittek, P. J.; Liao, J. K.; Cheng, C. C. *J. Org. Chem.* **1979**, *44*, 870.

(3) Kende, A. S.; Liebeskind, L. S.; Braitsch, D. M. *Tetrahedron Lett.* **1975**, 3375.

(4) Zembayashi, M.; Tamao, K.; Yoshida, J.; Kumada, M. *Tetrahedron Lett.* **1977**, 4089.

(5) Colon, I.; Kelsey, D. R. *J. Org. Chem.* **1986**, *51*, 2627.

(6) (a) Troupel, M.; Rollin, Y.; Perichon, J.; Fauvarque, J. F. *Nouv. J. Chim.* **1981**, *5*, 621. (b) Fauvarque, J. F.; Chevrot, C.; Jutand, A.; François, M.; Perichon, J. *J. Organomet. Chem.* **1984**, *264*, 273.

(7) (a) Troupel, M.; Rollin, Y.; Sibille, S.; Fauvarque, J. F.; Perichon, J. *J. Chem. Res. Synop.* **1980**, 26. (b) Schiavon, G.; Bontempelli, G.; Corain, B. *J. Chem. Soc., Dalton Trans.* **1981**, 1074.

(8) Fauvarque, J. F.; Petit, M. A.; Pflüger, F.; Jutand, A.; Chevrot, C.; Troupel, M. *Makromol. Chem., Rapid Commun.* **1983**, *4*, 455.

(9) (a) Parshall, G. W. *J. Am. Chem. Soc.* **1974**, *96*, 2360. (b) Hidai, M.; Kashiwagi, T.; Ikenchi, T.; Uchida, Y. *J. Organomet. Chem.* **1971**, *30*, 279. (c) Fahey, D. R. *J. Am. Chem. Soc.* **1970**, *92*, 402. (d) Fahey, D. R. *Organomet. Chem. Rev., Sect. A* **1972**, *7*, 245. (e) Fahey, D. R.; Mahan, J. D. *J. Am. Chem. Soc.* **1977**, *99*, 2501.

(10) (a) Tsou, T. T.; Kochi, J. K. *J. Am. Chem. Soc.* **1979**, *101*, 6319. (b) *Ibid.* **1979**, *101*, 7547. (c) *J. Org. Chem.* **1980**, *45*, 1930.

(11) See, e.g., ref 5, pp 2632–2633, or ref 10b, pp 7552–7554, for detailed presentations of the main mechanistic sequences proposed in the literature.

0276-7333/88/2307-2203$01.50/0

Scheme II

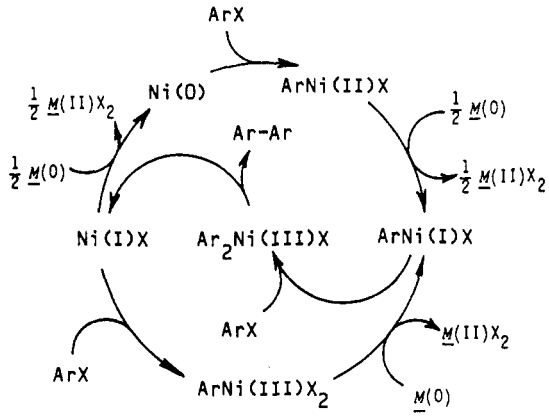

Most of the mechanisms proposed involve metathesis of the arylnickel(II).[9a,12] However, elegant mechanistic work, by Tsou and Kochi[10b] led to the conclusion that the biaryl formation involves a radical chain process in which paramagnetic nickel(I) and arylnickel(III) are the reactive intermediates. This suggests that under homogeneous catalytic conditions a double-chain mechanism is operative as sketched in Scheme I, although the mechanism was originally established under stoichiometric conditions.

Recent work by Colon and Kelsey,[5] although not supported by a full mechanistic analysis, also considered the intermediacy of Ni(I) and Ni(III) species. Yet owing to the presence of an excess of reducing metal, the key step is postulated to be the electron-transfer activation of $ArNi^{II}X$ to the corresponding Ni(I) species which oxidatively adds to the organic halide. Thus the mechanism in Scheme II[5] proposes also a double-chain sequence that interacts competitively at the level of Ni(I) intermediates rather than cooperatively as in the Tsou and Kochi's mechanism in Scheme I. The overall chains are triggered by the initial formation of Ni(0) intermediate via reduction of the Ni(II) salt. Yet it must be emphasized at this point that the experimental conditions were sufficiently diverse (excess of reducing agent in the case of Scheme II; $ArNi^{II}X$ as the starting material in the establishment of Scheme I) in both studies to consider that different mechanisms may operate for each condition. Indeed in the absence of an excess of reductant it is unlikely that the mechanism in Scheme II can operate efficiently. On the other hand, the mechanism in Scheme I requires a bimolecular step (eq 6) involving two species present in trace concentrations

$$ArNi^{III}X_2 + ArNi^{II}X \rightarrow Ar_2Ni^{III}X + Ni^{II}X_2 \quad (6)$$

under the conditions found in catalytic reactions such as those leading to the proposal of Scheme II. Thus, under these latter conditions such a step may not be sufficiently rapid to compete efficiently with the direct reduction of the two reacting intermediates in eq 6 to the common arylnickel (I) species. In our opinion, the mechanistic sequences in Schemes I and II are not to be viewed as opposite but rather as two limiting sequences whose relative importance is a function of the exact experimental conditions: Scheme I being favored in the presence of large amounts of nickel catalyst and Scheme II being favored in the presence of small amounts of nickel but excess of homogeneous reductant.

Alternative mechanisms have been postulated on the basis of semiquantitative electrochemical data and all agree

(12) Matsumoto, H.; Inaha, S.-I.; Rieke, R. D. *J. Org. Chem.* **1983**, *48*, 840.

Scheme III

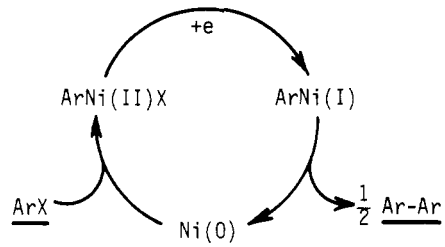

Scheme IV

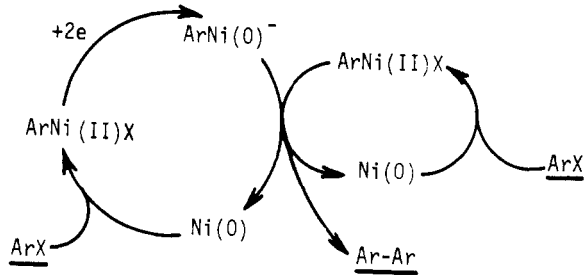

Scheme V

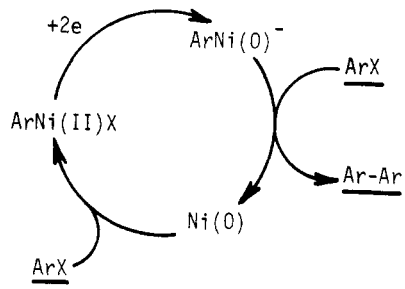

on the fact that the key intermediate is the arylnickel(II) species formed by oxidative addition of the organic halide to the electrogenerated Ni(0). Reduction of this species leads to a large enhancement of the biaryl formation rate in agreement with the above presentation and Scheme II, yet various interpretations have been proposed as summarized in Schemes III–V, depending on the number of electrons considered for the electrochemical reduction of the arylnickel(II) species. Indeed Scheme III[7b] supposes that the reduction involves a single electron transfer to afford the arylnickel(I) intermediate operative in Scheme II. However, in contrast with Scheme II it is assumed that the latter reacts with itself to afford the biaryl and Ni(0) species. Schemes IV[7b] and V[7a,b] consider that a two-electron reduction takes place to yield an anionic arylnickel(0) intermediate that reacts with the arylnickel(II) or the organic halide to afford the biaryl while regenerating the zerovalent nickel. Yet to the best of our knowledge, there are no conclusive experimental evidence that arylnickel(II) intermediates may be reduced through a two-electron step.[13] Indeed Bontempelli and co-workers[7b] report that $PhNi(PPh_3)_2Br$ reduction involves a one-electron consumption in the absence of purposely added bromobenzene, under exhaustive electrolysis conditions.

Besides discrepancies in the interpretation of the actual mechanism of biaryl formation from aryl halides in the

(13) (a) It is reported[7b] that $PhNi(PPh_3)_2Br$ reduction under voltammetric reduction involves two successive monoelectronic waves. Yet no indication of such a behavior has been observed in the present study with $PhNi(PPh_2CH_2CH_2PPh_2)Br$ (vide infra). (b) Preparative scale electrolysis of $PhNi^{II}XL_2$ involves[7a] a two-electron consumption. This corresponds to a gross reaction and does not demonstrate that the initial reduction occurs via a 2e uptake.

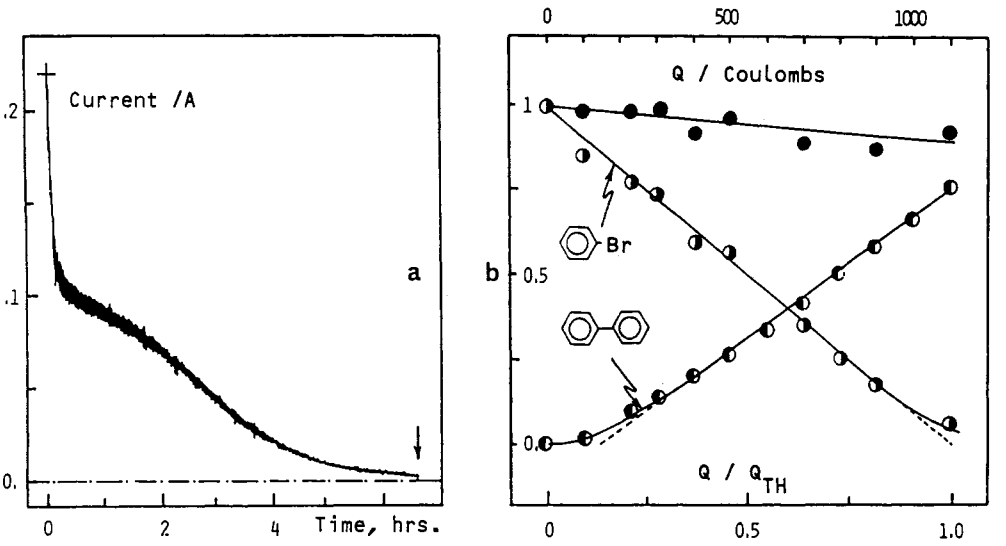

Figure 1. Preparative electrolysis of PhBr (9.3 mmol) in the presence of $NiCl_2$(dppe) (1 mmol) in a HMPA/THF (1/2) mixture (0.1 M NBu_4BF_4) at 20 °C: (a) variations of the electrolysis current with time; the arrow indicates the end of electrolysis; (b) variations of the solution composition normalized to the initial PhBr, as a function of the charge, Q, consumed. Q_{TH} = theoretical charge consumption for 1 e/PhBr: (◑), unreacted PhBr; (◐), biphenyl; (●), mass balance including PhBr, PhPh, and phenylnickel derivatives.

presence of nickel, all the reported mechanisms have in common the initial formation of an arylnickel(II) halide from nickel(0) and the organic halide. It is generally considered that the oxidative addition of aryl halides to nickel(0) complexes is rapid. However, quantitative data are scarce in the literature and are related to the reaction of stable Ni^0L_3 complexes.[14] On the other hand, electrochemical methods have proved efficient for the in situ generation of coordinatively unsaturated zerovalent complexes via reduction of their divalent parents (eq 7).

$$M^{II}X_2L_2 + 2e^- \rightarrow 2X^- + \text{“}M^0L_2\text{”} \rightarrow \ldots \quad (7)$$

Such poorly ligated zerovalent metals are indeed more reactive than their coordinatively saturated analogues.[15] For example, Ni^0(dppe) (dppe = 1,2-bis(diphenylphosphino)ethane) obtained from reduction of $NiCl_2$(dppe) is more efficient in the electrocarboxylation of aromatic halides[6b] or in the electropolymerization of *p*-dibromobenzene to poly-*p*-phenylene[8] than the saturated $Ni^0(PPh_3)_4$. Noteworthy the saturated analogue $Ni^0(dppe)_2$ is stable but is totally unreactive[9b,17a] toward the same halides.

In the present study we wish to demonstrate that the recent availability of microelectrodes, allowing fast scan cyclic voltammetry[18] in highly resistive solvents such as THF, is a convenient method for the determination of the kinetics of oxidative addition of organic halides to coordinatively unsaturated zerovalent nickel complexes. Furthermore, we wish to show that significant data can be obtained by the same method to interpret the mechanism of catalytic biaryl formation by Ni(0) under reductive conditions, i.e. for conditions in which the coupling reagents involve an excess of a reducing metal (Zn, Mg, ...) and catalytic amounts of phosphine nickel complexes. Indeed, electrochemical methods, allowing fine variations of the reducing properties of the electrode, as well as a precise determination of the kinetics occurring in the solution afford valuable kinetic information that would otherwise be difficult to obtain. On the other hand, the observed kinetics are not to be viewed as being characteristic of electrochemical conditions. Indeed, although initiated at the electrode, the various chemical events take place in the solution, i.e. in conditions akin to those met under nonelectrochemical situations.

Results

Preparative electrolysis at the mercury pool of a solution in a HMPA/THF (1/2) mixture of bromobenzene (9.3 mmol) and $NiCl_2$ (dppe) (1 mmol) at −2 V vs SCE results in the formation of biphenyl (10% unreacted bromobenzene, 75% faradaic yield, 85% chemical yield) according to the balance equation (8). Benzene was not

$$2PhBr + 0.2NiCl_2(dppe) \xrightarrow[-2\ V\ vs\ SCE]{+2.4\ e;} PhPh + 2Br^- + 0.2\ \text{“Ni...”} \quad (8)$$

$$0.2NiCl_2(dppe) \xrightarrow[\geq -1.8\ V\ vs\ SCE]{+0.4\ e;} 2PhBr + 0.2\ \text{“Ni...”} \quad (9)$$

formed in any significant amounts under these reaction conditions. Figure 1 presents the variations of the electrolysis current and of those of the solution composition with time. During the first stage of the electrolysis the current drops to ca. 45% of its initial value to reach a plateau from which it decays slowly to zero. The fast initial drop, which involves the uptake of ca. 2 e/Ni(II), is comparable to the current variations with time observed in the absence of PhBr or in the presence of PhBr when the electrolysis is performed at potentials less cathodic than −1.8 V vs SCE. During the first stage PhBr is consumed

(14) (a) Reference 10a, p 6322. (b) Troupel, M.; Rollin, Y.; Sibille, S.; Fauvarque, J. F.; Perichon, J. *J. Chem. Res., Synop.* **1980**, 24.

(15) The rate of oxidative addition of PhI to $Pd^0(PPh_3)_2$ is at least 10^5 faster than that to $Pd^0(PPh_3)_4$.[16] Amatore, C.; Azzabi, M.; Jutand, A., manuscript in preparation.

(16) Fauvarque, J. F.; Pflüger, F. *J. Organomet. Chem.* **1981**, *208*, 419.

(17) (a) Sock, O.; Troupel, M.; Perichon, J.; Chevrot, C.; Jutand, A. *J. Electroanal. Chem.* **1985**, *183*, 237. (b) Reduction of $Ni^{II}Br_2$(dppe) involves, as for the chloride analogue, two one-electron waves yielding respectively Ni^IBr(dppe) at $E_p^{R'1} = -0.65$ V vs SCE (at 0.2 V·s^{-1}) and Ni^0(dppe) at $E_p^{R'2} = -1.32$ V vs SCE (at 0.2 V·s^{-1}). The peak location of the two waves, although close to that observed for the chloride analogue, are significantly less cathodic. Similarly, the role of the coordination shell of the nickel on the complex electronic properties is also evidenced by the lower rate constant ($k \approx 10^3$ M^{-1} s^{-1}) measured for the dimerization of Ni^IBr(dppe).

(18) (a) In cyclic voltammetry the characteristic time domain, θ, is related to the scan rate through[19] $\theta = (RT/n\mathcal{F}v)$, i.e., for a monoelectronic process at room temperature $\theta \approx (25/v)$ ms where v is expressed in V·s^{-1}. (b) Amatore, C. A.; Jutand, A.; Pflüger, F. *J. Electroanal. Chem.* **1987**, *218*, 361.

(19) (a) Amatore, C.; Gareil, M.; Savéant, J.-M. *J. Electroanal. Chem.* **1983**, *147*, 1. (b) Amatore, C.; Savéant, J.-M. *J. Electroanal. Chem.* **1983**, *144*, 59.

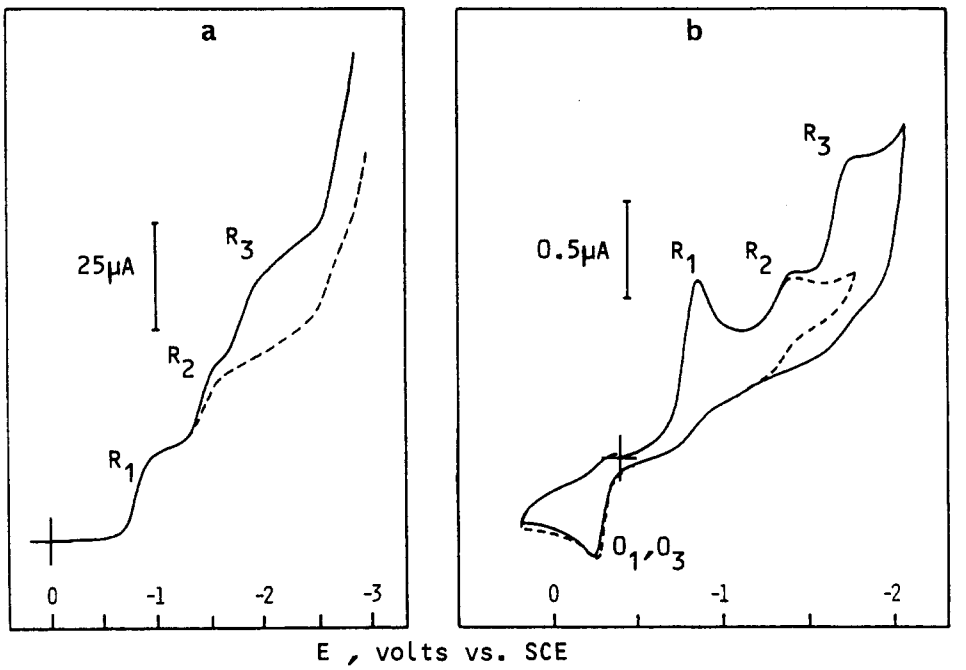

Figure 2. Cyclic voltammetry of $NiCl_2(dppe)$ (2 mM) in the same medium as in Figure 1, alone (dashed curves) or in the presence of 1 equiv of PhBr (solid curves): (a) gold rotating disk (ϕ = 2 mm; ω = 105 rad·s^{-1}; v = 20 mV·s^{-1}) electrode; (b) stationary gold disk microelectrode (ϕ = 0.5 mm; v = 200 mV·s^{-1}) at 20 °C.

but no biphenyl is produced (compare Figure 1b). HPLC chromatography of the solution electrolyzed at $E > -1.8$V vs SCE indicates that the bromobenzene is essentially unreacted, except for the formation of arylnickel species, and that only 2 e/Ni(II) are consumed. Thus the reducing power of the electrode is crucial to the success of the biaryl synthesis, in eq 8, during the time duration (few hours) of the laboratory scale electrolysis. When the electrode potential is not sufficiently cathodic, the electrolysis amounts only to reduce the Ni(II) catalyst, the solution turning progressively black. On the other hand at sufficiently cathodic potential (−2 V/SCE) the solution stays clear up to the very end of the electrolysis, and bromobenzene is catalytically converted to biphenyl.

In order to rationalize this dependence on the electrolysis potential, it is important to examine first the electrochemical behavior of Ni(II) in the absence and in the presence of bromobenzene.

I. Cyclic Voltammetry of $Ni^{II}Cl_2(dppe)$. Cyclic voltammetry at the rotating disk electrode shows that $Ni^{II}Cl_2(dppe)$ is reduced in two successive waves of nearly identical plateau values at $E_{1/2}$ = −0.77 and −1.36 V vs SCE, respectively, which are ascribed to the following processes:[17a]

$$Ni^{II}Cl_2(dppe) + e \rightarrow Ni(I) + ... \quad (10)$$

$$Ni^{II}Cl_2(dppe) + 2e \rightarrow Ni(0) + ... \quad (11)$$

Transient cyclic voltammetry at the stationary disk electrode in Figure 2 indicates that the monoelectronic reduction in eq 10, occurring at wave R_1, yields a nickel species which is too unstable to be reduced quantitatively at the potential of the second reduction wave R_2. Indeed the current magnitude of the R_2 wave is considerably smaller than that of wave R_1 when cyclic voltammetry is performed at moderate scan rates[18a] and depends on the initial nickel complex concentration. Yet when shorter time scales are considered, current magnitude of wave R_2 is progressively restored and reaches that of wave R_1 for scan rates above 500 V·s^{-1}, i.e. $\theta < 50$ μs as evidenced by the voltammograms in Figure 3a and the variations of $i^P_{R_2}/i^P_{R_1}$, the current peaks ratio of wave R_2 relative to wave R_1, with the ratio $v/C°$, in Figure 3b. Such behavior indicates that the Ni(I) species formed in eq 10 evolves through a second-order reaction.[20] On the other hand the linear variations (slope 0.48, correlation coefficient = 0.99) of log ($i^P_{R_1}/S$) with log v in Figure 4 establishes[20] that the mechanism and the number of electrons (1e) corresponding to the first reduction wave, R_1, remains unchanged within all the time-scale domain investigated (1–25 s).

The above behavior demonstrates that the nickel(I) complex formed at the chemically irreversible reduction wave R_1 evolves to yield an electroinactive dimeric species with a rate constant of 2.5 × 10^3 M^{-1} s^{-1}.[21] Such a behavior stems certainly from the low coordination state of the nickel(I) formed in eq 12. Indeed in the presence of added phosphine the electrochemical system of waves R_1 and R_2 is completely different.[17a] Within a shorter time scale (v > 500 V·s^{-1}) the unsaturated nickel(I) is reduced irreversibly at wave R_2 before it can react in reaction 13.

$$Ni^{II}Cl_2(dppe) + e^- \rightarrow Ni^{I}Cl(dppe) + Cl^- \quad (12)$$

$$2Ni^{I}Cl(dppe) \rightarrow \text{dimer} \quad (13)$$

From the curve in figure 3b, a half-life of few milliseconds is estimated for the unsaturated Ni(I) under our experimental conditions. Its monoelectronic reduction wave, R_2 establishes that it can be further reduced to the nickel(0) state (eq 14). Noteworthy, even at the highest

$$Ni^{I}Cl_2(dppe) + e^- \rightarrow Ni^{0}(dppe) + Cl^- \quad (14)$$

(20) (a) Bard, A. J.; Faulkner, L. R. In *Electroanalytical Methods*; Wiley: New York, 1980. (b) Andrieux, C. P.; Savéant, J. M. In *Investigation of Rates and Mechanism of Reactions*; Bernasconi, C. F., Ed.; Wiley: New York, 1986; Vol. 6, 4/E, Part 2, pp 305–390.

(21) (a) See, e.g.: Corain, B.; Bressan, M.; Rigo, P.; Turco, A. *Chem. Commun.* **1968**, 509. Aresta, M.; Nobile, C. F.; Sacco, A. *Inorg. Chim. Acta* **1975**, *12*, 167, for analogue dimeric nickel(I) species. (b) Vide infra and footnote 33 for the determination of the rate constant of nickel(I) dimerization. (c) The concentration dependence in Figure 3b (note the $C°$ factor on the lower and upper scales) excludes any pseudo-first-order pathway in the Ni(I) chemical fate; see, e.g.: Amatore, C.; Garreau, D.; Hammi, M.; Pinson, J.; Savéant, J.-M. *J. Electroanal. Chem.* **1985**, *184*, 1 and ref 20.

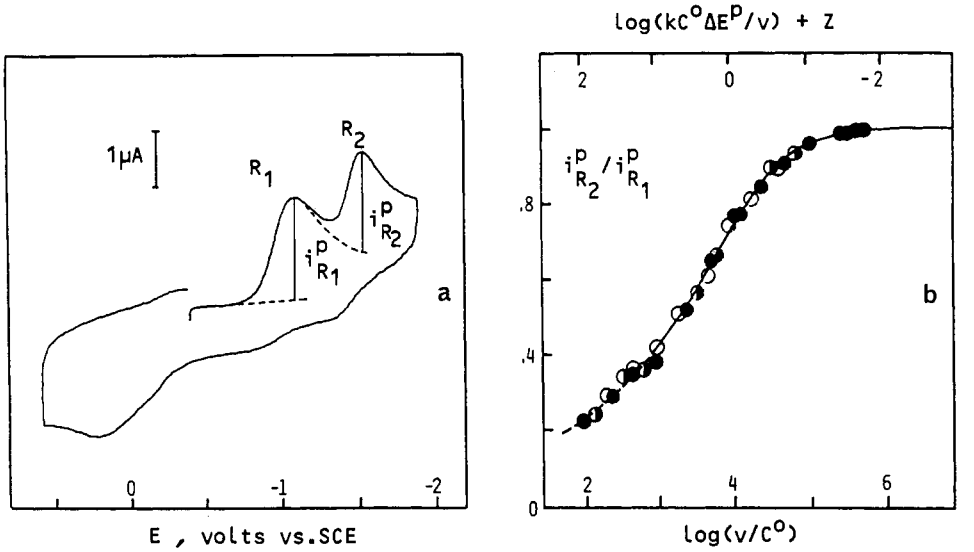

Figure 3. (a) Cyclic voltammetry of $NiCl_2(dppe)$ (2 mM) in the same medium as in Figure 1. Voltammogram at a stationary gold microelectrode (ϕ = 125 μm, v = 500 V·s^{-1}). (b) Variations of the current peak ratio $i^p_{R_2}/i^p_{R_1}$ with the scan rate, v, and the nickel(II) concentration, C^0: (○) 1.0, (◑) 1.5, and (●) 2.0 mM. Solid line: theoretical variations for a Ni(I)/Ni(I) dimerization mechanism (see text and footnote 33) (v in V·s^{-1}; C^0 in M, ΔE^p in V; k in M^{-1} s^{-1}; $Z = 0.034(F\Delta E^p/RT)$; 20 °C).

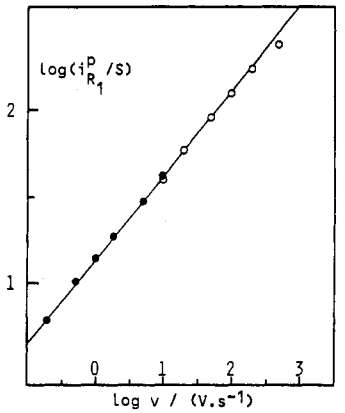

Figure 4. Variations of the current peak density of the first reduction wave (R_1) of $NiCl_2(dppe)$ in the same conditions as in Figure 3, as a function of the scan rate, v, at stationary gold disk microelectrodes: (●) ϕ = 1.5 mm, S = 1.8 mm^2; (○) ϕ = 0.5 mm; S = 0.20 mm^2. The current density is expressed in arbitrary units (0.55 μA·mm^{-2}).

scan rates investigated (v = 5000 V·s^{-1}), waves R_1 and R_2 remain totally irreversible and are associated with the broad reoxidation peak O_1 in Figures 2 and 3. This shows that the overall successive one-electron transfers occurring at waves R_1 and R_2 are not reversible and are accompanied by a fast reorganization of the coordination shells leading presumably to halide loss. Finally, we want to point out that, even at the lowest scan rates used (0.1 V·s^{-1}), no evidence of the disproportionation reaction (15) has been obtained. Indeed if such a reaction were to occur, the peak height of wave R_1 should tend to that corresponding to a two-electron process when v is decreased.[22]

$$2Ni^{I}Cl(dppe) \rightarrow Ni^{0}(dppe) + Ni^{II}Cl_2(dppe) \quad (15)$$

(22) The rate constant of the disproportionation reaction 15 can be estimated to be close to $k \approx k_{dif} \exp F(E^\circ_{Ni(II)/Ni(0)} - E^\circ_{Ni(II)/Ni(I)})/RT$ where k_{dif} is the diffusion rate limit ($\sim 3 \times 10^9$ M^{-1} s^{-1}).[23] Owing to the irreversible nature of waves R_1 and R_2 their standard potential difference is not measurable. Yet an estimate based on the difference of peak potentials (–0.56 V at v = 0.2 V·s^{-1}) gives $k \sim 1$ M^{-1} s^{-1} which would correspond to a half-life of ca. 10^3 s in the conditions of Figure 3, i.e., much larger than the nonredox process in eq 13.

(23) Bard, A. J.; Kojima, H. *J. Am. Chem. Soc.* **1975**, *97*, 6317.

II. Cyclic Voltammetry of $Ni^{II}Cl_2(dppe)$ in the Presence of Bromobenzene. A. In the Presence of 1 Equiv of Bromobenzene. In the presence of 1 equiv of bromobenzene, the waves R_1 and R_2 remain unchanged in position and current magnitude, indicating that within the time scale of cyclic voltammetry, the Ni(I) species formed upon one-electron intake from $Ni^{II}Cl_2(dppe)$ does not react with the bromobenzene (eq 16). However, when

$$Ni^{I}Cl(dppe) + PhBr \not\rightarrow \ldots \quad (16)$$

the scan is extended cathodically, a new wave, R_3, develops around –1.8 V vs SCE, as shown in Figure 2b. The same experiment performed at the rotating disk electrode in Figure 2a indicates that wave R_3 involves the net consumption of one electron since its current plateau is nearly identical[24] with that of wave R_1.

At the stationary disk electrode the growth of wave R_3 is concomitant with that of an oxidation wave, O_3 (E_p = –0.25 V vs SCE at 0.2 V·s^{-1}) which develops at the expense of the wave O_1 (E_p = –0.28 V vs SCE at 0.2 V·s^{-1}) previously observed in the absence of purposely added bromobenzene. Both waves R_3 and O_3 correspond respectively to the reduction and the oxidation of the phenylnickel(II) $PhNi^{II}Br(dppe)$, resulting from the fast oxidative addition of PhBr to the low ligated $Ni^0(dppe)$ electrogenerated at wave R_2. Indeed the cyclic voltammetry of an independently prepared phenylnickel(II) complex is identical with that observed above.[25]

(24) This is further confirmed by the one-electron limit for wave R_3 in cyclic voltammetry for the larger scan rates, when the electrode is initially polarized on the plateau of wave R_2. See later and compare Figure 7b.

(25) $PhNi^{II}Br(dppe)$ was prepared according to the method[26] previously described for the analogue $PhPd^{II}I(dppe)$ and summarized in eq 17 and 18 and characterized by its ^1H NMR and IR spectra.[27]

$$Ni^{II}Cl_2(PPh_3)_2 + dppe \xrightarrow{2EtMgBr} (PPh_3)_2Ni^0(dppe) \quad (17)$$

$$(PPh_3)_2Ni^0(dppe) + PhBr \rightarrow PhNi^{II}Br(dppe) + 2PPh_3 \quad (18)$$

(26) (a) Fauvarque, J. F.; Jutand, A. *Bull. Soc. Chim. Fr.* **1976**, 765. (b) Fauvarque, J. F.; Jutand, A. *J. Organomet. Chem.* **1979**, *177*, 273.

(27) Analogues of the $PhNi^{II}Br(dppe)$ have been previously described from the reaction of (perchlorobenzene)magnesium chloride with $Ni^{II}Cl_2(dppe)$: Coronas, J. M.; Rossell, O.; Sales, J. *J. Organomet. Chem.* **1975**, *97*, 473.

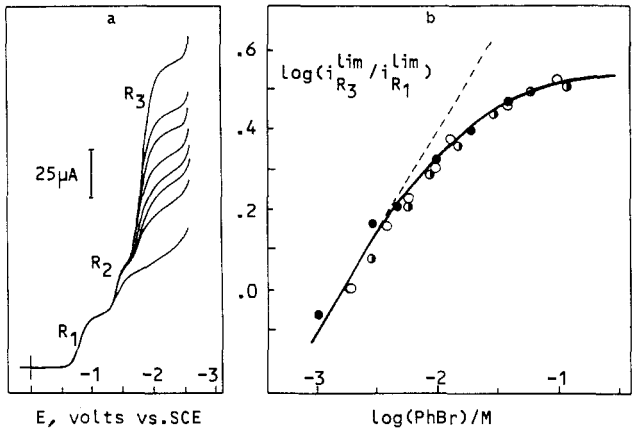

Figure 5. Cyclic voltammetry of $NiCl_2(dppe)$ in the same conditions as in Figure 3 at a rotating disk electrode (ϕ = 2 mm; ω = 105 rad·s^{-1}; v = 20 mV·s^{-1}) in the presence of various amounts of PhBr (from bottom to top: 0, 1, 2, 3, 5, 10, 20, and 50 equiv): (a) cyclic voltammograms, (b) variations of $n = i^{lim}_{R_3}/i^{lim}_{R_1}$, the apparent number of electrons consumed at wave R_3, as a function of the bromobenzene concentration and of the nickel(II) concentration: (●) 1.0, (○) 2.0, and (◑) 3.0 mM.

The rotating disk voltammogram in Figure 2b thus demonstrates that the zerovalent nickel formed at wave R_2 readily inserts into the carbon–bromide bond of bromobenzene to afford quantitatively the phenylnickel(II) complex in eq 19. The same result is obtained from cyclic

$$Ni^0(dppe) + PhBr \rightarrow PhNi^{II}Br(dppe) \qquad (19)$$

voltammetry at the stationary disk electrode when the initial potential of the electrode is cathodic to the reduction peak R_2. However, when cyclic voltammetry is performed starting from an initial potential anodic to wave R_1, the current magnitude of wave R_3 is dependent on the scan rate as well as one the bromobenzene concentration (see later) because part of the Ni(I) formed at R_1 evolves through reaction 13.

B. In the Presence of Excess of Bromobenzene. Figure 5 presents the voltammograms obtained at the rotating disk electrode, for the reduction of $Ni^{II}Cl_2(dppe)$ in the presence of various amounts of added bromobenzene. The waves R_1 and R_2 featuring the successive one-electron reduction steps of Ni(II) into Ni(I) and Ni(0), respectively, remain strictly proportional to the initial concentration of the $Ni^{II}Cl_2(dppe)$ complex and are not affected by the bromobenzene concentration. Thus even at the larger concentrations (0.1 M) of bromobenzene no indication of reaction with Ni(I) is obtained within the time scale investigated. In sharp contrast, the wave R_3 increases with the bromobenzene concentration. As shown by the plot in Figure 5b, the apparent number of electrons, n, consumed at wave R_3, i.e., its limiting current value normalized to that of wave R_1, is only a function of PhBr concentration and independent of the initial concentration of the nickel complex. A linear dependence with $[PhBr]^{1/2}$ is observed for the smaller values of bromobenzene concentration. Yet a leveling effect is observed when the latter reaches the 0.1 M concentration range, indicating a change in the rate-determining step of the overall kinetics.

The enhancement of wave R_3 in the presence of excess of bromobenzene is typical of a catalytic mechanism regenerating[28] continuously the arylnickel(II) complex and

(28) See, e.g.: (a) Nicholson, R. S.; Shain, I. *Anal. Chem.* **1964**, *36*, 706. (b) Andrieux, C. P.; Blocman, C.; Dumas-Bouchiat, J.-M., M'Halla, F.; Savéant, J. M. *J. Am. Chem. Soc.* **1980**, *102*, 3806 and references therein. (c) Hershberger, J. W.; Amatore, C.; Kochi, J. K. *J. Organomet. Chem.* **1983**, *250*, 345.

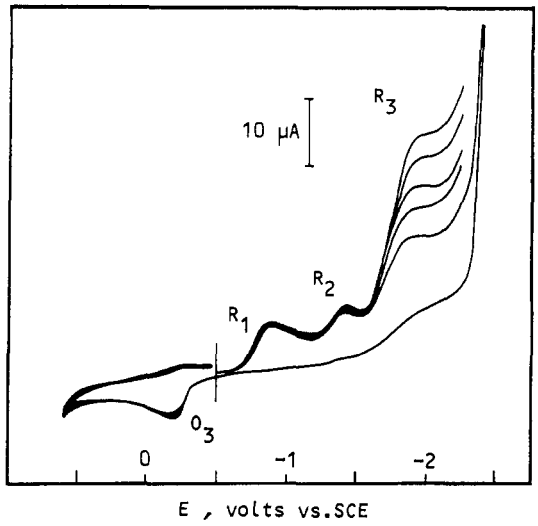

Figure 6. Cyclic voltammetry of an identical solution as that in Figure 5 (stationary gold disk microelectrode: ϕ = 1.5 mm; v = 200 mV·s^{-1}) in the presence of various amounts of PhBr (from bottom to top: 5, 7, 10, 21, and 31 equiv).

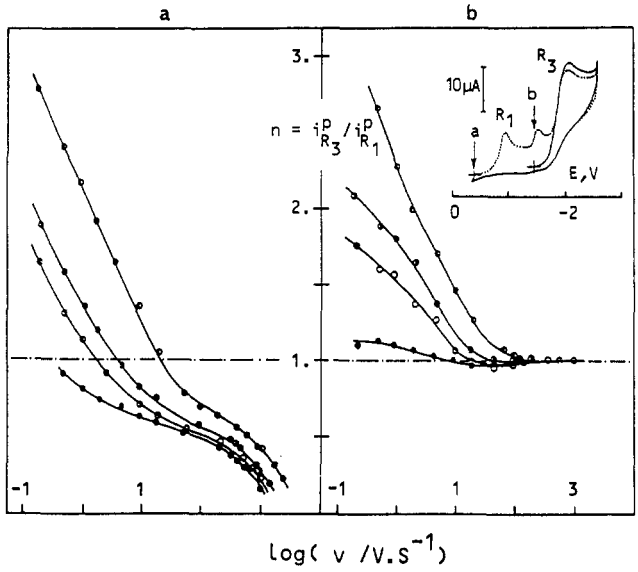

Figure 7. Variations of the apparent number, $n = i^P_{R_3}/i^P_{R_1}$, of electrons consumed at wave R_3 in cyclic voltammetry at the stationary gold disk electrode (ϕ = 1.5 mm), as a function of the scan rate, v, and of the bromobenzene excess factor: (●) 1, (○) 2, (◑) 3, and (◐) 5 equiv, for the same solution as in Figure 3. The electrode rest potential was set at −0.4 V vs SCE in (a) or at the foot of wave R_3 in (b) as indicated by the corresponding arrows on the voltammogram (v = 500 mV·s^{-1}; 5 equiv of PhBr) shown in the insert.

is consistent with the behavior observed above upon large-scale electrolysis of the same solutions (compare the efficient biphenyl synthesis at −2 V vs SCE and the negligible yields at E > −1.8 V vs SCE) (eq 20).

$$PhNi^{II}Br(dppe) + e^- \longrightarrow \ldots \xrightarrow{PhBr} \ldots PhNi^{II}Br(dppe) + \ldots \qquad (20)$$

A similar increase of the R_3 wave is observed in cyclic voltammetry at the steady disk electrode, upon addition of bromobenzene to the $Ni^{II}Cl_2(dppe)$ solution as illustrated by the voltammograms in Figure 6. It is noteworthy that waves R_1 and R_2 remain invariant with the bromobenzene concentration. By contrast the height of the reduction wave R_3 of $PhNi^{II}Br(dppe)$ depends on the scan rate (v) and on the bromobenzene concentration. Moreover, the plot in Figure 7a shows that the R_3 wave does

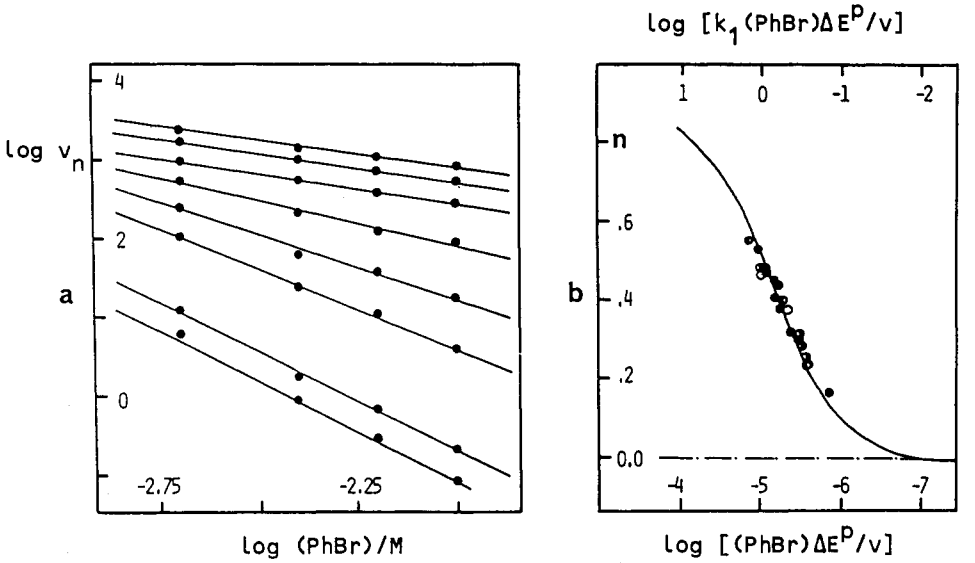

Figure 8. (a) Variations of v_n with PhBr concentration, as a function of n. See text for the definitions of n and v_n. From top to bottom n = 0.2 (1.0), 0.3 (1.0), 0.4 (1.0), 0.5 (1.35), 0.6 (2.0), 0.7 (2.5), 1.25 (3.2), and 1.5 (3.2), the numbers between parentheses being the slopes of the lines in (a). (b) Unified plot of the data in Figure 7a as a function of PhBr concentration and scan rate, v, for $n \leq 0.55$. See text and footnote 32 for the derivation of the theoretical variations represented in solid line ((PhBr) in M; v in V·s^{-1}, ΔE^p in V; k_1 in M^{-1}·s^{-1}).

not vary monotonically with the scan rate. This is clear evidence that the current magnitude of wave R_3 is controlled at least by two different chemical steps intervening sequentially when the scan rate is increased, i.e., when the time scale is decreased.

Finally, in order to investigate the eventual role of the bromide ions released during the electron-transfer chain process in eq 8 and 20, an identical set of experiments was repeated in the presence of purposely added excesses of $NBu_4^+Br^-$, comparable to bromobenzene concentration. No significant effect on the magnitude of wave R_3 was observed, the latter being identical with that observed in the absence of added bromide ions within the accuracy of the measurements.[29]

$PhNi^{II}Br(dppe)$ was generated in situ by setting the rest potential of the electrode cathodic to the second reduction wave, R_2, of $Ni^{II}Cl_2(dppe)$ in the presence of various amounts of bromobenzene. The resulting variations of the current peak of the reduction wave R_3 of the arylnickel(II) complex with the scan rate and the bromobenzene excess are shown in Figure 7b. At low scan rates the currents observed are similar to those measured in the conditions of Figure 7a. However, for higher scan rates, the current tends toward a limit corresponding to the one-electron reduction in eq 21. The observation of this limit corresponds to the suppression of the regenerating mechanism in eq 20. Thus the variations below unity of the apparent number of electrons consumed in Figure 7a are related to the rate of insertion of the $Ni^0(dppe)$, electrogenerated at wave R_2, into the carbon–bromide bond of the bromobenzene.[30] This is further supported by the dependence of log v_n vs log [PhBr] in Figure 8a, where v_n is the scan rate such as the number of electrons exchanged at wave R_3 is n ($0 < n < 1$). Indeed the slope of the variations in Figure 8a tends toward unity for the lower values of n, i.e., when the catalytic regeneration in eq 20 no longer interferes. Such a value establishes[31] that the formation of $PhNi^{II}Br(dppe)$ obeys the chemical kinetic law in eq 22.

$$PhNi^{II}Br(dppe) + e^- \rightarrow PhNi^{I}(dppe) + Br^- \quad (21)$$

$$d[PhNi^{II}Br(dppe)]/dt = k_1[Ni^0(dppe)][PhBr] \quad (22)$$

Thus the data in Figure 7a, for $n \leq 0.55$, are replotted in Figure 8b, as a function of the single parameter $\Delta E^p \cdot [PhBr]/v$ which enables us to evaluate[32] the rate constant of the oxidative addition of bromobenzene to the coordinatively unsaturated zerovalent nickel in reaction 23 ($k_1 = 10^5$ M^{-1} s^{-1}).

$$PhBr + Ni^0(dppe) \xrightarrow{k_1} PhNi^{II}Br(dppe) \quad (23)$$

Discussion

I. Electrochemical Generation of Coordinatively Unsaturated Zerovalent Nickel $Ni^0(dppe)$. Electrochemical reduction of divalent nickel complexes such as $Ni^{II}Cl_2(dppe)$ occurs through two successive monoelectronic processes to afford successively coordinatively unsaturated nickel(I) and nickel(0) complexes in eq 24 and 25. The monovalent nickel electrogenerated at the first

$$Ni^{II}Cl_2(dppe) \xrightarrow{+e\,-\,Cl^-} Ni^{I}Cl(dppe) \quad (24)$$

$$Ni^{II}Cl_2(dppe) \xrightarrow{+2e\,-\,2Cl^-} Ni^{0}(dppe) \quad (25)$$

reduction wave undergoes a rapid dimerization, with a rate constant of 2.5×10^3 M^{-1} s^{-1},[33] to afford a nonelectroactive

(29) Compare ref 5, p 2630.

(30) In the scan rate domain where the apparent number of electron exchanged at wave R_3 falls below unity in Figure 7a, the initial $Ni^{II}Cl_2$(dppe) is quantitatively reduced to Ni^0(dppe), the deactivation of Ni^ICl(dppe) being suppressed (compare Figure 3b).

(31) See, e.g., ref 19b and: Aalstadd, B.; Ronlan, A.; Parker, V. D. *Acta Chem. Scand., Ser. B* **1981**, *B35*, 649 and references therein.

(32) (a) The "working curve" in Figure 8b is adapted from the original data by R. S. Nicholson and I. Shain in ref 28, which gives the percent of reversibility of an EC voltammogram as a function of the time ellapsed. (b) For the situation under consideration, the time ellapsed in $\Delta E_p/v$, where ΔE_p is the difference between the peak potentials of waves R_1 and R_2. (c) The original working curves were derived for electrochemical situations in which the initial electron transfer is reversible, i.e., for conditions different of the ones investigated in this paper. However, since only relative variations of peak currents are considered, this introduces only slight uncertainties in the rate constant measured. Further confirmation of the correctness of the method is given by the small dispersions in the experimental data in Figures 3 and 8.[44]

dimer. However, provided the time scale of the transient electrochemical method is short enough, the monovalent nickel species is reduced to the zerovalent nickel, before its facile dimerization can occur. In the absence of suitable reactant the nickel(0) thus obtained evolves to yield metallic nickel and coordinatively saturated zerovalent nickel according to the stoichiometry[17a] in eq 26.

$$2Ni^0(dppe) \rightarrow Ni + Ni^0(dppe)_2 \qquad (26)$$

II. Mechanism and Rate of Oxidative Addition to Ni^0(dppe). In the presence of bromobenzene no colloidal nickel(0) formation is observed, indicating the facile reaction of the unsaturated zerovalent nickel with the organic halide. This reaction corresponds to the oxidative addition of bromobenzene to Ni^0(dppe) in eq 27, as shown by the

$$Ni^0(dppe) + PhBr \xrightarrow{k_1} PhNi^{II}Br(dppe) \qquad (27)$$

concomittant growth of the $PhNi^{II}Br$(dppe) reduction wave (compare Figures 5 and 6). The rate constant of the oxidative addition is evaluated to be 10^5 M^{-1} s^{-1} by cyclic voltammetry, i.e. ~50 000 times larger than that of coordinatively saturated analogues such as $Ni^0(PEt_3)_3$[14a] and about 5 000 000 times larger than that corresponding to $Ni^0(PPh_3)_3$.[14b] This dramatic increase emphasizes the considerable reactivity of unsaturated nickel compared to that of usual nickel catalysts, Ni^0P_4 (P = phosphine). The value of the second dissociation equilibrium constant, K_2, in eq 28 is estimated to be smaller than 10^{-6} M, whereas

$$Ni^0(PPh_3)_4 \overset{K_1}{\rightleftharpoons} Ni^0(PPh_3)_3 + PPh_3 \overset{K_2}{\rightleftharpoons} Ni^0(PPh_3)_2 + 2PPh_3 \qquad (28)$$

that of the first dissociation equilibrium is larger than 10^2 M.[10a] Then, if the reactive species is considered to be the bis(phosphine)nickel(0) species, its rate constant is at least one thousand times larger than the apparent rate (for millimolar concentration of nickel zerovalent), a result in good agreement with our above determination.

Thus electrochemical generation of Ni(0) from reduction of millimolar Ni(II) complexes serves to create the Ni^0P_2 reactive species at millimolar concentrations whereas the latter is present at submicromolar to nanomolar concentrations when the catalyst is introduced as its chemically stable form Ni^0P_4.

III. Mechanism of Biaryl Synthesis with Electrochemically Activated Nickel Complexes. Paramagnetic Nickel Complexes as the Intermediates. Exhaustive electrolysis of bromobenzene in the presence of divalent nickel $Ni^{II}Cl_2$(dppe) affords excellent yields of biphenyl provided that electrolysis is performed at sufficiently cathodic potentials ($E \approx -2.0$ V vs SCE).

The transient electrochemical data obtained via cyclic voltammetry in Figure 7a identify at least two different limiting steps as a function of the time scale. In the microsecond time scale, the oxidative addition of the bromobenzene to Ni^0(dppe) limits the formation of the $PhNi^{II}Br$(dppe) in eq 27. Yet in the millisecond time scale this process is too fast to be responsible for the limitation of the turnover number observed in Figures 5b and 7b.[28] More direct evidence for the involvement of at least two sequential steps is given by the dramatic change of curvatures in Figure 7a. In the following we will discuss the nature of these steps that occur after the oxidative addition.

(33) A procedure similar to that described in footnote 32 was used to derive the working curve in Figure 3b, for determination of $k = 2.5 \times 10^8$ M^{-1} s^{-1}. The original theoretical data were taken from: Olmstead, M. L.; Hamilton, R. G.; Nicholson, R. S. *Anal. Chem.* **1969**, *41*, 260.

Scheme VI

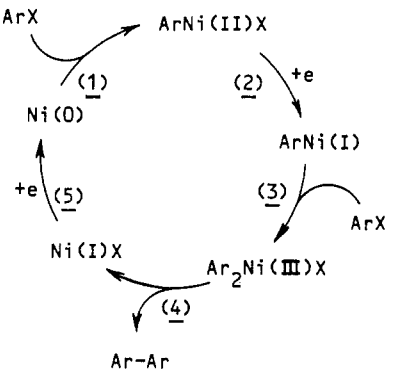

We wish first to delineate the monoelectronic reduction of the phenylnickel(II) bromide to afford the paramagnetic nickel(I) species in eq 29.[34] The one-electron consumption is clearly established by the limit of one electron observed at large scan rates in Figure 7b, although in contradiction with previous reports[7] of two-electron reduction for related species.

$$PhNi^{II}Br(dppe) \xrightarrow[-Br^-]{+e} PhNi^{I}(dppe) \qquad (29)$$

The variations, with the bromobenzene concentration, of the overall number of electrons consumed during the reduction of $PhNi^{II}Br$(dppe) at the rotating disk electrode demonstrates that PhBr is involved (in addition to the initial insertion reaction with Ni^0(dppe)) in the catalytic regeneration of $PhNi^{II}Br$(dppe) in eq 20. From the slope of the plot in Figure 5b at the lower values of [PhBr], the corresponding reaction involves PhBr and a nickel complex with a molecularity of one for each.[38] On the other hand, since no dependence with the nickel concentration is observed, no bimolecular step involving nickel-centered intermediates is involved in the propagation of the catalytic sequence in eq 20.[40]

On the basis of this kinetic evidence we propose the mechanism in Scheme VI as a description of the catalytic process responsible for biphenyl formation, occurring at the reduction wave of the $ArNi^{II}$(dppe)Br.[41]

Note that the catalytic cycle in Scheme VI corresponds to the upper route[42] of the catalytic cycle postulated by

(34) The arylnickel(II) complex is also oxidized by a monoelectronic process: The mechanism of anodic oxidation of $PhNi^{II}Br$(dppe) is currently under investigation and will be reported separately. Similar observations have already been reported for analogue complexes with monodentate phosphines.[14b] Compare ref 35–37.

(35) Almemark, M.; Akermark, B. *J. Chem. Soc., Chem. Commun.* **1978**, 66.

(36) (a) Morrell, D. G.; Kochi, J. K. *J. Am. Chem. Soc.* **1975**, *97*, 7262. (b) With triethylphosphine electrochemical oxidation of the arylnickel(I) halide affords excellent yields of arylphosphonium salt: Tsou, T. T.; Kochi, J. K. *J. Am. Chem. Soc.* **1978**, *100*, 1634.

$$ArNi^{II}X(PEt_3)_2 \xrightarrow{-e} ArNi^{III}X(PEt_3)_2 \xrightarrow{fast} Ar^+PEt_3 + Ni^IX$$

(37) For stable arylnickel(III) complexes see, e.g.: (a) Grove, D. M.; van Koten, G.; Zoet, R. *J. Am. Chem. Soc.* **1983**, *105*, 1379. (b) Grove, D. M.; van Koten, G.; Mul, W. P.; van der Zeijden, A. A. H.; Terheijden, J.; Zoutberg, M. C.; Stam, C. H. *Organometallics* **1986**, *5*, 322.

(38) The slope of 0.5 observed in Figure 5b corresponds to a molecularity of unity for bromobenzene, for electrochemical experiments under steady-state conditions[39] such as rotating disk cyclic voltammetry. This dependence originates from the second-order differential nature of Fick's kinetics equations.[20]

(39) Amatore, C.; Savéant, J.-M. *J. Electroanal. Chem.* **1981**, *123*, 189.

(40) Compare ref 10a, where such a bimolecular step has been identified:

$$ArNi^{III}X_2 + ArNi^{II}X \rightarrow Ni^{II}X_2 + Ar_2Ni^{III}X$$

(41) The dppe ligand is omitted for simplification. All the nickel species in Scheme VI are supposed to be coordinated by a dppe ligand.

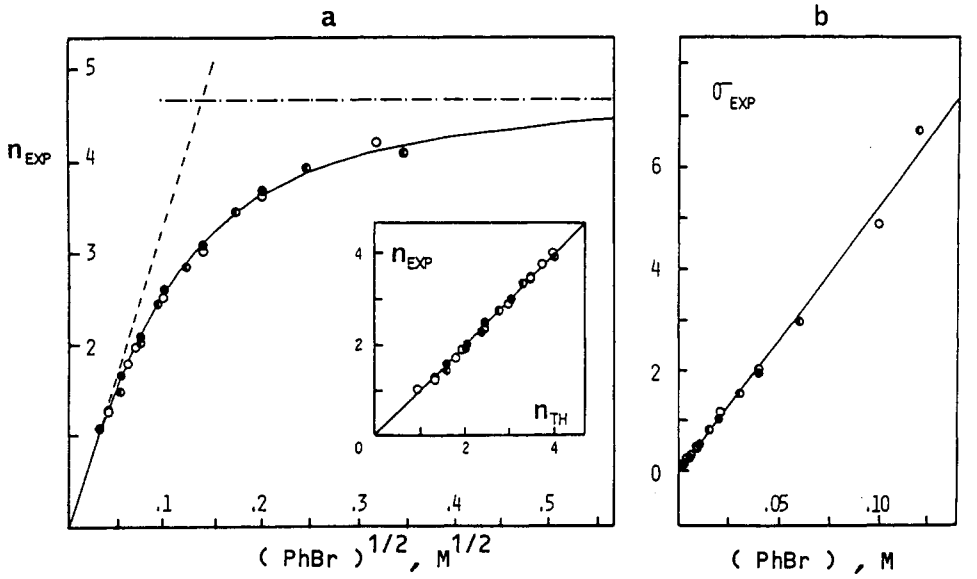

Figure 9. (a) Plot of the data in Figure 5 as a function of the PhBr concentration. The solid line corresponds to eq 30. The experimental (n_{EXP}) and theoretical (n_{TH}) values of the apparent number of electron consumed are compared in the insert. (b) Plot of the same data under the form in eq 33.

Colon et al.[5] (see Scheme II) where the homogeneous reductions of $Ni^{I}X$ and $ArNi^{II}X$ are replaced by the heterogeneous reduction at the electrode.

Scheme VI involves no bimolecular step between catalytic species, a requirement from the above kinetic observation and a favorable condition for a fast propagation of the overall cycle. Furthermore some of the steps involved (steps 1, 2, and 5) have been characterized independently in the present study. Two additional steps are involved in addition on the basis of kinetic requirements: oxidative addition of bromobenzene to $ArNi^{I}(dppe)$[37,43] in step 3 to afford the diarylnickel(III) species which is known to undergo a rapid reductive elimination[5,10b,35,36a] in step 4. In the following we wish to establish that the quantitative kinetic treatment of the mechanism in Scheme VI is in remarkable agreement with the data obtained in Figure 5b at the rotating disk electrode.

For the catalytic sequence in Scheme VI, the reduction steps 2 and 5 are not rate-determining when the electrode potential is set on the arylnickel(II) reduction wave R_3. Similarly the oxidative addition of bromobenzene to $Ni^{0}(dppe)$ is sufficiently fast not to be involved in the kinetic control of the propagation kinetics except within the shortest time scales. Thus the apparent number of electrons, n, consumed at wave R_3 in Figure 5 is controlled by the reactions in steps 3 and 4. Resolution of the pertinent diffusion reaction equations[44] shows that n is given in eq 30 as a function of [PhBr], where k_3 and k_4 are the

$$n = 2[\mathrm{PhBr}]^{1/2}(k_3\delta^2/D)^{1/2}[1 + (k_3[\mathrm{PhBr}]/k_4)^{1/2}]/[1 + (k_3[\mathrm{PhBr}]/k_4)^{1/2} + (k_3[\mathrm{PhBr}]/k_4)] \quad (30)$$

rate constants of steps 3 and 4, respectively, δ is the diffusion layer thickness, and D is the average diffusion coefficient of the different nickel species. Such an expression predicts a linear dependence with $[\mathrm{PhBr}]^{1/2}$ at low bromobenzene concentration ($[\mathrm{PhBr}] \ll (k_4/k_3)$), i.e., when the oxidative addition of PhBr to $PhNi^{I}(dppe)$ is rate-limiting (eq 31). In the converse situation, n is in-

$$[\mathrm{PhBr}] \ll (k_4/k_3) \qquad n \approx 2(k_3\delta^2/D)^{1/2}[\mathrm{PhBr}]^{1/2} \quad (31)$$

$$[\mathrm{PhBr}] \gg (k_4/k_3) \qquad n \approx 2(k_4\delta^2/D)^{1/2} \quad (32)$$

dependent of the bromobenzene concentration which corresponds to the reductive elimination in step 4 being the rate-determining step (eq 32). Such a behavior is in qualitative agreement with the observations in Figure 5b of linear variation of n with $[\mathrm{PhBr}]^{1/2}$ at low [PhBr] and of the leveling effect at higher concentrations of bromobenzene. Thus, when the data in Figure 5b are replotted as a function of $[\mathrm{PhBr}]^{1/2}$ in Figure 9a, the deviations from the initial slope of 33.7 $M^{-1/2}$ can be evaluated as $\alpha = (33.7[\mathrm{PhBr}]^{1/2}/n) - 1$ where [PhBr] is expressed in M. On the other hand, rewriting eq 30 gives α as a function of [PhBr] in eq 33. A plot of the left-hand side of eq 33 as

$$\sigma_{exp} = [\alpha + (\alpha^2 + 4\alpha)^{1/2}]^2/4 = k_3[\mathrm{PhBr}]/k_4 \quad (33)$$

a function of [PhBr] in Figure 9b establishes the validity of eq 33 and thus of eq 30 and allows the determination of $k_3/k_4 = 52.5\ M^{-1}$. On the other hand, $k_3 = 960\ M^{-1}\ s^{-1}$ is obtained from the initial slope value of 33.7 $M^{-1/2}$,[45] from which it ensues that $k_4 = 18\ s^{-1}$. Introduction of these rate constants values into eq 30 allows the theoretical value of n to be determined as a function of the bromobenzene

(42) The lower route in Scheme II is ruled out in our conditions since within our time scale $Ni^{I}Br(dppe)$ is not sufficiently reactive toward PhBr to allow the catalytic cycle to propagate. Indeed $Ni^{I}X(dppe)$ reduction wave is invariant even in presence of the largest concentrations (0.1 M) of PhBr. Compare Figure 6 and ref 43.

(43) (a) For precedent of such reaction see ref 5, 10b, and 10c and: Gosden, C. G. Healy, K. P.; Pletcher, D. *J. Chem. Soc., Dalton Trans.* **1978**, 972. (b) It is apparently surprising that $Ni^{I}X(dppe)$ does not react appreciatly with PhBr although $PhNi^{I}(dppe)$ is considered sufficiently reactive to allow the fast propagation of the catalytic cycle in Scheme VI. We ascribe this change of reactivity to the replacement of the halogen ligand by the phenyl. Indeed, the reactivity of Ni(I) complexes is known to highly depend on the nature of its ligands, even for minor change such as chloride/bromide exchange. See, e.g.: ref 21 a and: Lovecchio, F. V.; Gore, E. S.; Busch, D. H. *J. Am. Chem. Soc.* **1974**, *96*, 3109. (c) The rate of the oxidative addition is reported (see, e.g.: ref 10a) to increase greatly with the ease of ArX reduction. Thus it appears that an increase of the reducing character of the Ni(I) species should result in the same trend. Although direct measurement was not possible in this study, it seems reasonable that the presence of a phenyl ligand in $PhNi^{I}(dppe)$ results in an increase of the electron donor properties of the Ni(I) complex. (d) Compare footnote 17b and the fact that $PhNi^{II}Br(dppe)$ is reduced ca. 1.1 V more cathodically than $Ni^{II}Br_2(dppe)$.

(44) Amatore, C.; Mottier, L.; Jutand, A., manuscript in preparation.

(45) $k_3 = 285(D/\delta^2)\ M^{-1}\ s^{-1}$ where D is in $cm^2\ s^{-1}$ and δ in cm. Determination of $D = 2.8 \times 10^{-6}\ cm^2\ s^{-1}$ is made by calibration with ferrocene ($D = 7.3 \times 10^{-6}\ cm^2\ s^{-1}$) in cyclic voltammetry and $\delta = 9.1 \times 10^{-4}$ cm from the current plateau of the Ni(II)/Ni(I) reduction wave R_1 at the rotating disk electrode.

concentration in Figure 9a. Comparison of the experimental values of n with the latter in the insert in Figure 9a further confirms the experimental validity of the mechanism in Scheme VI and of the rate constants thus determined.[46]

To conclude this section, we wish to discuss the mechanism in Scheme VI in connection with previously proposed mechanisms for catalytic biaryl synthesis by nickel complexes. As stated above the mechanism in Scheme VI is identical with the upper route in Scheme II postulated by Colon and Kelsey[5] on the basis of kinetic observations and product distribution. On the other hand, although involving paramagnetic nickel(I) and nickel(III) intermediates akin to that first proposed by Tsou and Kochi,[10b] the mechanism in Scheme VI is quite different from that proposed in Scheme I. Our interpretation is that the difference is related to the presence, in our experiments, of a large reductive driving force (the cathode) which allows the rather difficult reductions in steps 2 and 5 to be performed easily. In the absence of such a driving force,[10b] the mechanism in Scheme VI cannot operate efficiently as shown by the absence of sizeable catalytic effect when the electrode potential is not set on the reduction wave of the arylnickel(II) complex (vide supra).

Summary and Conclusion

Biphenyl synthesis proceeds from electrogenerated coordinatively unsaturated nickel(0) by a chain process involving nickel(I) and nickel(III) intermediates as well as nickel(0) and nickel(II) complexes. The various steps allowing the catalytic chain in Scheme VI to propagate have been identified and their rate constants or redox characteristics determined either independently or from the general treatment of the overall chain kinetics, eq 34–38 (peak potentials refers to SCE and correspond to 0.2 V·s^{-1}).

$$\mathrm{PhBr} + \mathrm{Ni^0(dppe)} \xrightarrow{\text{step 1}} \mathrm{PhNi^{II}Br(dppe)} \qquad k_1 = 1.1 \times 10^5\ \mathrm{M^{-1}\ s^{-1}} \tag{34}$$

$$\mathrm{PhNi^{II}Br(dppe)} + \mathrm{e} \xrightarrow{\text{step 2}} \mathrm{PhNi^{I}(dppe)} + \mathrm{Br^-} \qquad E_p^2 = -1.75\ \mathrm{V} \tag{35}$$

$$\mathrm{PhBr} + \mathrm{PhNi^{I}(dppe)} \xrightarrow{\text{step 3}} \mathrm{Ph_2Ni^{III}Br(dppe)} \qquad k_3 = 960\ \mathrm{M^{-1}\ s^{-1}} \tag{36}$$

$$\mathrm{Ph_2Ni^{III}Br(dppe)} \xrightarrow{\text{step 4}} \mathrm{Ph\text{-}Ph} + \mathrm{Ni^{I}Br(dppe)} \qquad k_4 = 18\ \mathrm{s^{-1}} \tag{37}$$

$$\mathrm{Ni^{I}Br(dppe)} + \mathrm{e} \xrightarrow{\text{step 5}} \mathrm{Ni^0(dppe)} + \mathrm{Br^-} \qquad E_p^5 = -1.32\ \mathrm{V}^{17b} \tag{38}$$

The chain is initiated by two successive single-electron transfers (eq 39) to the divalent nickel $\mathrm{Ni^{II}Cl_2(dppe)}$ to afford the true catalytic species $\mathrm{Ni^0(dppe)}$ which enters the cycle in Scheme VI, step 1 (E refers to peak potentials vs SCE at 0.2 V·s^{-1}).

$$\mathrm{Ni^{II}Cl_2(dppe)} \xrightarrow[-0.81\ \mathrm{V}]{+\mathrm{e}\ -\ \mathrm{Cl^-}} \mathrm{Ni^{I}Cl(dppe)} \xrightarrow[-1.38\ \mathrm{V}]{+\mathrm{e}\ -\ \mathrm{Cl^-}} \mathrm{Ni^0(dppe)} \tag{39}$$

Thus, when considered as a whole, the mechanism of biphenyl synthesis from organic halides, catalyzed by nickel(II) complexes under reducing conditions (the cathode in this study or a reducing metal[4,5]), involves a double series of electron-transfer steps;[47] (i) those in reaction 39 which activate the catalyst and (ii) those in eq 35 and 38 which are essential to the fast propagation of the catalytic chain. Among these electron-transfer steps, one that requires the largest cathodic potential ($E < -1.8$ V vs SCE) is the monoelectronic reduction of the inert phenylnickel(II) complex to the reactive phenylnickel(I) in reaction 35. In the absence of a large reductive driving force, this step is then certainly the rate-determining reaction in the propagation of the chain. In this respect it must be emphasized at this point that the electrochemical results presented in this study do not have a finality per se. Indeed electrochemistry simply affords a convenient and accurate mean of controling the reducing driving force in eq 35, 38, and 39 (through a precise and continuous tuning of the cathode potential) as well as the kinetics of the reactions following these reductions (through the current flow at the cathode). Thus electrochemical methods permit an easy approach to the investigation of the crucial role (compare e.g. ref 4 and 5 and references therein) of the reducing metals used in more conventional experiments on the success of biaryl synthesis by transition-metal activation of carbon–halogen bonds. Similarly, the chemical steps characterized in this study (eq 13, 34, 36, 37), although monitored by electrochemical means, occur in solution in conditions that are akin to those encountered when reducing metals are used instead of an electrode.[48] Thus the mechanistic conclusions and rate constants should be transposable to usual conditions when care is taken of eventual medium changes.

When the biaryl synthesis is performed with the metal powder as the reducing agent, the electron transfer in reaction 35 is certainly the slowest step in the chain sequence. This results in the fact that most of the nickel catalyst is "stored" in the form of an arylnickel(II) intermediate. Thus the instant concentration of the inorganic nickel(I) species $\mathrm{Ni^{I}(dppe)}$ is extremely low, which acts as a "protection" of the catalyst vis-à-vis its consumption via the rapid dimerization of $\mathrm{Ni^{I}X(dppe)}$ identified in this study (reaction 40, $k = 2.5 \times 10^3\ \mathrm{M^{-1}\ s^{-1}}$) that would otherwise rapidly deactivate the catalytic cycle.[49] A second

$$2\mathrm{Ni^{I}Cl(dppe)} \rightarrow \text{dimeric nickel} \tag{40}$$

(46) The current variations in Figure 7a involve the time convolution of three processes: (i) formation of Ni(0) by reduction of $\mathrm{Ni^{II}Cl_2}$; (ii) oxidative addition of PhBr to Ni(0); (iii) propagation of the chain in Scheme VI. The time dependence of each of these individual mechanisms has been observed independently in Figures 3b, 8b, and 7b, respectively. It is thus seen than the variations in Figure 7a are in qualitative agreement with the above decomposition when a simple time-independent convolution is used: $n = n(\mathrm{i})n(\mathrm{ii})n(\mathrm{iii})$, where n is the apparent number of electron consumed at wave R_3 in Figure 7a, n(i) that at wave R_2 in Figure 3a, n(ii) that in Figure 8b, and n(iii) that in Figure 7b. However, quantitative kinetic informations cannot be extracted from such a crude model, which neglects the time interdependence of the three processes and must await the derivation of the pertinent model (work currently in progress).

(47) Compare to the DAISET concept introduced in: Chanon, M., Tobe, M. L., *Angew. Chem., Int. Ed. Engl.* **1982**, *21*, 1. Chanon, M. *Bull. Soc. Chim. Fr.* **1982**, 197.

(48) The analogy between the microelectrodes used in this study and metal particles used in classical experiments is even deeper than one based upon a simple parallel of redox properties. Indeed, under stirred conditions, the solution is to be considered as homogeneous except within ca. 10 μm of the particle surface. In the latter region, because of hydrodynamics, a stagnant larger is established similarly to what happens in the close vicinity of an electrode.[20a] Within this layer (the "diffusion layer") the different chemicals involved diffuse to and from the particle surface, and concentration profiles, akin to those encountered at microelectrodes, develop. Owing to the relatively small variations of the diffusion layer thickness, δ, with normal stirring conditions, they are of comparable magnitude for microelectrodes (see part VII in the Experimental Section) and metal particles of dimensions larger than few 100 μm.

conclusion to be drawn is that when the coupling reagent involves catalytic amounts of nickel species and excess reducing metal, M, the conversion rate should obey the rate law in eq 41. k_M is a pseudorate constant depending on the

$$d[Ar-Ar]/dt = -d[ArX]/dt = k_M A_M[ArNi^{II}XL_2] \quad (41)$$

ease of reduction of $ArNi^{II}XL_2$, on the metal nature, on the hydrodynamics of the solution, and on the reactor volume. A_M is the overall active surface area of the metal, i.e., related to the metal "concentration" for a given distribution of particle sizes. Such a rate law is valid up to the very end of the biphenyl synthesis, that is, up to the point where bromobenzene concentration drops below the level at which oxidative additions to Ni(I) and Ni(0) become rate-limiting. Yet owing to the large magnitude of the rate constants in reactions 34 and 36, this should occur only in the latest stages of the organic halide conversion.

Since, from the above analysis, the nickel catalyst is almost entirely under the form of the arylnickel(II) species, the concentration of the latter is nearly identical with that, ["Ni"], of the catalyst. Thus eq 41 rewrites as eq 42 which

$$d[Ar-Ar]/dt = -d[ArX]/dt \approx k_M A_M["Ni"] \quad (42)$$

shows that the conversion rate (i) is of "zeroth" order in the organic halide, i.e., independent of the conversion yield, (ii) is proportional to the nickel concentration, (iii) increases with the "concentration" of reducing metal, through an increase of A_M, and (iv) finally should greatly depend on k_M, that is, on the metal nature and the ease of $ArNi^{II}XL_2$ reduction as well as on any additive that would facilitate the electron transfer in eq 35, via inner-sphere contributions. Interestingly all four effects have been observed by Colon and Kelsey (compare Figures 1–4 and Tables II and V in ref 5) and led these authors to correct, although no quantitative, deductions on the mechanism.[5]

In the following we wish to comment on the reactivity of zerovalent or monovalent nickel species vis-à-vis the oxidative addition of an aryl halide. In regard to zerovalent nickel, the results presented in this study demonstrate the dramatic role of the coordination shell on the rate of oxidative addition. Indeed, the unsaturated zerovalent nickel complexes Ni^0(dppe), inserts about 10 000 to several millions times faster than its saturated analogues Ni^0P_3 (P = PEt_3 or PPh_3). Although recognized previously (see, e.g., ref 10a) these effects were difficult to quantify mainly because of the almost impossible determination of the equilibrium constant of the phosphines dissociation in eq 43. In this respect electrochemistry proved to be very useful in allowing the bypassing of this equilibrium by direct generation of the reactive moiety Ni^0P_2.

$$Ni^0P_4 \rightleftarrows Ni^0P_3 + P \rightleftarrows Ni^0P_2 + 2P \quad (43)$$

In the above study, we used only a single bis(phosphine) ligand, so no information on the role of the ligand electronic properties is obtained for the zerovalent nickel species. However, this is thoroughly documented topic in the literature. Indeed it is established that the greater the donating properties of the ligand, the faster the oxidative addition. The same trend is observed in this work for oxidation to a monovalent nickel complex. In fact Ni^IX(dppe) (X = halide) proved to be unreactive vis-à-vis bromobenzene (up to 0.1 M) even within time scales of several seconds, whereas $PhNi^I$(dppe) reacts with a rate constant of ca. 10^3 M^{-1} s^{-1}. Thus a difference of reactivity of at least 1000 is introduced by the change from a halide to an aryl ligand. Although difficult to rationalize on a quantitative basis[43] such a dramatic effect is paralleled with the large increase (by ca. 1.1 V) in the reduction potentials when $Ni^{II}Br_2$(dppe) and $PhNi^{II}Br$(dppe) are considered. This shows the considerable role of the ligand Ph or X on the electron-transfer properties of the metal center. Though the effect of a corresponding change for Ni(I) species was not measured in this work, it is certainly of comparable magnitude as shown by the variation in reduction potentials (~60 mV) of Ni^IX(dppe) when X is a chloride or a bromide.[17b]

Experimental Section

I. Materials. Solvents THF and Et_2O were dried and distilled from sodium–benzophenone. HMPA was distilled from CaH_2. Bromobenzene was commercial and purified by distillation. $NiCl_2$(dppe) was prepared according to a described procedure.[50]

Instruments employed in this study were Perkin-Elmer Model IR 450 infrared spectrophotometer, Brucker WH 80 spectrometer for ^1H NMR spectra, and LKB 2152 for HPLC analyses. The preparative electrosynthesis was carried out with a Solea-Tacussel potentiostat PRT 4Q-1X. The same instrument was used for cyclic voltammetry at the rotating disk electrode. Cyclic voltammetry at the steady disk electrode was performed with a homemade ultrafast potentiostat,[51] with positive feedback ohmic drop compensation and a wave-form generator, PAR Model 175. The cyclic voltammograms were recorded with a Nicolet 3091 digital oscilloscope.

All experiments were carried out under anhydrous conditions at 20 °C. The cells were air-tight and were deoxygenated with argon on a vacuum Schlenk line.

II. Synthesis of PhNiBr(dppe). EtMgBr (2 mmol, 0.874 N in Et_2O) was added at 0 °C to 15 mL of Et_2O containing 0.53 g (1 mmol) of $NiCl_2$(dppe) and 0.526 g (2 mmol) of PPh_3. After 30 min at 0 °C, 0.5 mL (4.7 mmol) of PhBr was added. The mixture was stirred for 2 h at room temperature. The yellow precipitate was separated by filtration and solubilized with 20 mL of chloroform. Addition of petroleum ether precipitated yellow crystals that were dried under vacuum (0.47 g, 76% yield): mp 230–235 °C dec; IR (KBr pellet), characteristic IR vibrations of the ligand dppe (cm^{-1}), ν(C—$H_{arom.}$) 3055, ν(C—$H_{aliph.}$) 2940, 2900, ν(C=C) 1490, 1440, 1420, ν(=CH), 775, 740, 700, ν(C—C), 530, 510; characteristic IR vibrations of phenyl ligand to nickel (cm^{-1}), ν(C=C) 1595, 1420, ν(=CH) 765, 730; absence of the Ni–Cl stretching frequency at 330 cm^{-1} (present in the IR spectrum of the starting complex $NiCl_2$(dppe)) but presence of a band at 300 cm^{-1} assigned to the Ni–Br stretching frequency;[9b,52] ^1H NMR (80 MHz) 2.5 (m, 4 H, $-CH_2-$), 6.85–7.05 (m, 5 H), 7.2–7.8 ppm (m 20 H, arom H).

III. Preparative Electrosynthesis of Biphenyl. The electrosynthesis was carried out under argon at room temperature in a divided three-electrode cell with cathodic and anodic compartments separated by a sintered glass disk. The cathode was a 24 cm^2 mercury pool, while lithium was used as the anode. The reference electrode was a saturated calomel electrode connected to the solution through a 0.1 M nBu_4NBF_4, HMPA/THF (1/2) bridge. A mixture (65 mL) of HMPA/THF (1/2) and nBu_4NBF_4 (0.1 M) as a supporting electrolyte were introduced into the cathodic compartment while 20 mL of the same mixture was poured into the anodic compartment. Then 1 mL (9.28 mmol) of bromobenzene and 0.528 g (1 mmol) of the catalyst $NiCl_2$(dppe) were introduced into the cell.

(49) The main deactivation route observed in the preparative experiments in Figure 1 is related to the small quantities of benzene found at the end of the electrolysis when the bromobenzene concentration and current drop to zero. No hint of such deactivating route is observed during the kinetic experiments as shown by the perfect agreement of the experimental data with the mechanism in Scheme VI. Thus we are inclined to postulate that benzene is formed as a further evolution product of $PhNi^I$(dppe), competitive to bromobenzene oxidative addition. Such a path may be related to the intrinsic reactivity of $PhNi^I$(dppe) or rather to further reduction resulting from difficulties in controlling the electrode potential at the end of the electrolysis.

(50) Chatt, J.; Booth, G. *J. Chem. Soc.* **1965**, 3238.

(51) Howell, J. O.; Kuhr, W. G.; Ensman, R. E.; Wightman, R. M. *J. Electroanal. Chem.* **1986**, *209*, 77.

(52) Casabo, J.; Coronas, J. M.; Sales, J. *Inorg. Chim. Acta* **1974**, *11*, 5.

The electrolysis was conducted with a controlled potential of −2 V vs SCE. Every 100 C, 100-μL samples were withdrawn from the solution and analyzed by HPLC after addition of a known amount of bibenzyl as an internal standard. HPLC instrument was equipped with a reverse-phase column (RP 18, 5 μm, 250 × 4 mm). The eluant was a mixture of acetonitrile and water (60/40) containing 2% by weight of acetic acid. An UV detector set at 254 nm allowed the detection and measurements of PhH, PhBr, and PhPh present in the cell at different times of electrolysis. A ^{1}H NMR (80-MHz) spectrum on an aliquot after 200 C showed the presence of a multiplet at 6.85–7.05 ppm characteristic of the phenyl bonded to nickel in ca. 10% amount. No indication of free benzene in the reaction mixture was obtained. Yet after acidic hydrolysis, benzene was detected in the HPLC chromatogramm (1 mmol). In every aliquot, HPLC analysis gives approximately 1 mmol of benzene (arising from the acidic hydrolysis of 1 mmol of PhNiBr(dppe)) except at the end of the electrolysis where benzene was obtained in a slightly larger amount (see Figure 1b).[49]

IV. Voltammetry at the Rotating Disk Electrode. Experiments were carried out in a three-electrode cell. The counter electrode was a platinum wire; the reference was a saturated calomel electrode connected to the solution through a 0.1 M nBu_4NBF_4, HMPA/THF (1/2) bridge. The rotating electrode was a gold disk (ϕ = 2 mm) inserted into a Teflon holder (Tacusel EDI 65109).

A typical experiment was performed as follows: 40 mL of a HMPA/THF (1/2) mixture containing 0.1 M nBu_4NBF_4 was poured into the cell; 42 mg (2×10^{-3}M) of $NiCl_2$(dppe) was then added, and voltammetry was performed at the rotating disk electrode (angular velocity 105 rad·s^{-1}, Tacussel controvit) with a scan rate of 20 mV/s. Known amounts of PhBr (1–50 equiv/Ni) were added to the cell to examine the voltammetry, at the rotating disk electrode, of $NiCl_2$(dppe) in the presence of various amounts of PhBr. Analogous experiments were repeated at different $NiCl_2$(dppe) concentrations ((0.1 −3) × 10^{-3} M). The influence of the bromide concentration was studied on a solution containing, 2×10^{-3} M $NiCl_2$(dppe), 10^{-2} M PhBr, and various bromide concentrations by adding nBu_4NBr (from 2×10^{-3} to 1.2×10^{-2} M).

V. Voltammetry at the Stationary Disk Electrode. Experiments were carried out in a three-electrode cell. The counter electrode was a platinum gauze of ca. 1 cm^2 apparent surface area; the reference was a saturated calomel electrode connected to the solution through a 0.1 M nBu_4NBF_4, HMPA/THF (1/2) bridge. The working electrodes were gold disks made from cross sections of wires of various size (ϕ = 2 mm to 125 μm) sealed into glass, chosen according to the scan rate of the cyclic voltammetry to minimize ohmic drop effects.

Typical experiments were performed as follows: 15 mL of a HMPA/THF (1/2) mixture containing 0.1 M nBu_4NBF_4 was poured into the cell; 15.8 mg (2×10^{-3} M) of $NiCl_2$(dppe) was then added, and cyclic voltammetry was carried out at the stationary disk electrode at various scan rates from 0.1 to 5000 V·s^{-1}. Same experiments were repeated in the presence of PhBr (from 2×10^{-3} to 10^{-2} M).

VI. Determination of the Diffusion Coefficient of $NiCl_2$(dppe). At a rotating disk electrode the limiting current is given by[53]

$$i^{lim} = KFSC^0D^{2/3}$$

where $K = 0.620\, n\nu^{-1/6}\omega^{1/2}$, with ν being the kinematic viscosity of the solvent expressed in cm^2 s^{-1} and ω the angular velocity of the disk in rad·s^{-1}. Here the apparent number of electron exchanged is n = 1. ν is unknown so the diffusion coefficient of $NiCl_2$(dppe) was determined by comparison of the Ni(II)/Ni(I) reduction wave at a rotating disk electrode with that of ferrocene at the same electrode (one electron is involved in both cases). Thus

$$\frac{(i^{lim})_{Ni}}{(i^{lim})_{Fe}} = \frac{(C^0)_{Ni}}{(C^0)_{Fe}}\left(\frac{D_{Ni}}{D_{Fe}}\right)^{2/3}$$

It was necessary first to determine the diffusion coefficient of ferrocene. At a stationary disk electrode,[28a] $i^p = 0.446nFSC^\circ(DFv/RT)^{1/2}$. Voltammograms of ferrocene, 2.11×10^{-3} M, were recorded as a function of the scan rate v, at a stationary disk electrode (ϕ = 0.5 mm). Plotting i^p_{Fe} vs $v^{1/2}$ gives a straight line with a slope of 3×10^{-6} A (s.V^{-1})$^{1/2}$, for a concentration of 2.11×10^{-3} M. Since

$$i^p_{Fe} = 3 \times 10^{-6}v^{1/2} = 0.446FSC^0_{Fe}(D_{Fe}Fv/RT)^{1/2}$$

the value of D_{Fe} is obtained. The diffusion coefficient of ferrocene in the mixture HMPA/THF (1/2) containing 0.1 M nBu_4NBF_4 is thus determined to be $D_{Fe} = 7.3 \times 10^{-6}$ cm^2 s^{-1} (compare to the reported values of D_{Fe} in different nonprotic solvents ranging from 3×10^{-6} to 2×10^{-5} cm^2 s^{-1}).[54] $NiCl_2$(dppe), 2.15×10^{-3} M, was then added to the solution containing ferrocene (2.11×10^{-3} M). Voltammograms at the rotating disk electrode (ϕ = 2 mm) were performed on ferrocene and $NiCl_2$ (dppe) (first wave) with the same scan rate (20 mV·s^{-1}) and the same angular velocity (105 rad·s^{-1}). From the resulting limiting current values of 37 and 20 μA thus determined, respectively, it follows that $D_{Ni} = 0.39D_{Fe}$. The diffusion coefficient of $NiCl_2$(dppe) in the mixture HMPA/THF (2/1) containing 0.1 M nBu_4NBF_4 is then evaluated to be $D_{Ni} = 2.8 \times 10^{-6}$ cm^2 s^{-1}.

VII. Determination of the Diffusion Layer Thickness of $NiCl_2$(dppe) at the Rotating Disk Electrode (105 rad·s^{-1}). The limiting current observed at the rotating disk electrode is given by

$$i^{lim} = FSC^0D/\delta$$

where the diffusion layer thickness, δ, is proportional to $D^{1/3}$. Thus it ensues that

$$\delta_{Ni} = \delta_{Fe}(D_{Ni}/D_{Fe})^{1/3}$$

where

$$\delta_{Fe} = FSC^\circ_{Fe}D_{Fe}/i^{lim}_{Fe} = 12.5 \times 10^{-4} \text{ cm}$$

$$\delta_{Ni} = 91 \times 10^{-4} \text{ cm}$$

Acknowledgment. This work was supported in part by CNRS (Unité Associée UA 1110, Activation Moléculaire). Dr. Ian Jefferies is acknowledged for proofreading the manuscript before its submission.

Registry No. HMPA, 680-31-9; THF, 109-99-9; PhBr, 108-86-1; $Ni^{II}Cl_2$(dppe), 14647-23-5; $PhNi^{II}Br$(dppe), 115677-85-5; $PhNi^{I}$(dppe), 115677-86-6; $Ph_2Ni^{III}Br$(dppe), 115677-87-7; Ni^0(dppe), 96666-44-3; EtMgBr, 107-26-6; PPh_3, 603-35-0; biphenyl, 92-52-4.

(53) Heineman, W. R.; Kissinger, P. T. In *Laboratory techniques in Electroanalytical Chemistry*; Kissinger, P. T., Heineman, W. R., Eds.; Marcel Dekker: New York and Basel, 1984; p 115.

(54) Zara, A. J.; Machado, S. S.; Bulhoes, L. O. S.; Benedetti, A. V.; Rabockai, T. *J. Electroanal. Chem.* **1987**, *221*, 165.